

WAVES IN RADIAL GRAVITY USING MAGNETIC FLUID.

D. R. Ohlsen¹, J. E. Hart², and P. D. Weidman³,

¹Program in Atmospheric and Oceanic Sciences, University of Colorado, Boulder, CO 80309-0311,
ohlsen@fluida.colorado.edu

²Program in Atmospheric and Oceanic Sciences, University of Colorado, Boulder, CO 80309-0311,
hart@tack.colorado.edu

³Department of Mechanical Engineering, University of Colorado, Boulder, CO 80309-0427,
Patrick.Weidman@colorado.edu

INTRODUCTION

Terrestrial laboratory experiments studying various fluid dynamical processes are constrained, by being in an Earth laboratory, to have a gravitational body force which is uniform and unidirectional. Therefore fluid free-surfaces are horizontal and flat. Such free surfaces must have a vertical solid boundary to keep the fluid from spreading horizontally along a gravitational potential surface. In the absence of terrestrial gravity, surface tension forms fluid masses into spherical balls without solid boundaries, as demonstrated on the Space Shuttle in the Drop Physics Module [1]. A fundamentally different problem is the behavior of fluids with a *body* force rather than a surface force that generates the spherical geometry. In many atmospheric, oceanic, or stellar fluid flows, the horizontal scale is large enough that sphericity is important in the dynamics. Further, fluids in spherical geometry can cover an entire domain without any sidewall effects, i.e. have truly periodic boundary conditions. We describe novel spherical body-force laboratory experiments using ferrofluid.

Ferrofluids are dilute suspensions of magnetic dipoles, for example magnetite particles of order 10 nm diameter, suspended in a carrier fluid [2]. A surfactant coating keeps the particles separate so that thermal Brownian motions in the fluid are sufficient to overcome both gravity and particle-particle attraction to keep the dipoles in suspension. For flows in which external magnetic field variations and the bulk fluid motions are slow compared to the time for the magnetic fluid particles to rotate ($\sim 10^{-6}$ s), the fluid magnetization, \mathbf{M} , is parallel to the applied magnetic field, \mathbf{H} . If there is a gradient in $H = |\mathbf{H}|$, then there will be a systematic body force owing to the slight but persistent correlation of field strength and pole sense. With this additional body force term, the momentum equations become [2]:

$$\frac{d\mathbf{u}}{dt} + \mathbf{u} \cdot \nabla \mathbf{u} + 2\boldsymbol{\Omega} \times \mathbf{u} = -\frac{\nabla p}{\rho} + \mathbf{g} + \frac{M\nabla H}{\rho} + \nu \nabla^2 \mathbf{u} \quad (1).$$

The superparamagnetic ferrofluid response is complicated by the fact that $M = M(H)$ unlike ρ which is independent of g for the gravitational case. As the applied magnetic field, H , increases, more of the ferrofluid dipoles line up with the field resulting in a linear increase in ferrofluid magnetization, M , for small H but

saturation at M_s for large H . Figure 1 shows an example measurement of the field-averaged magnetization,

$$\bar{M} \equiv \frac{1}{H} \int_0^H M dH'$$

that shows this effect.

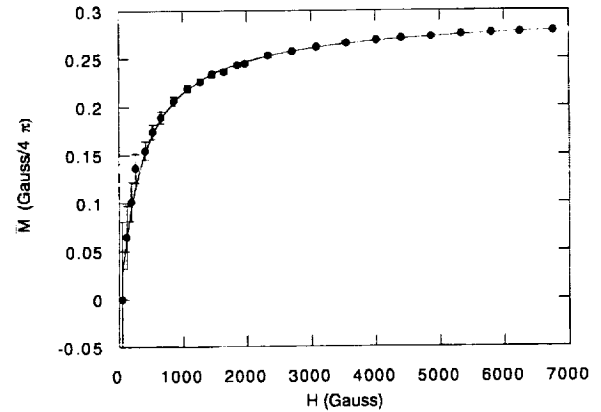


Figure 1. Field averaged magnetization vs. magnetic field for diluted water-based ferrofluid. The curve is a least-squares fit to a theoretical Langevin function prediction [2, 3].

In the experiments described below, the magnetic fields are less than 400 Gauss so M is nearly proportional to H . We have made careful measurements of M vs. H for $H < 500$ Gauss and fit them empirically to polynomials in H to use in theoretical predictions of the body force, $M\nabla H$.

APPROACH

The present study improves on the laboratory technique introduced in [3]. Figure 2 shows a schematic of the experiment. The apparatus is cylindrically axisymmetric. A cylindrical ceramic magnet is embedded in a smooth, solid, spherical PVC ball. The body force on the water-based ferrofluid depends only on the field strength and gradient from the interior magnet. The geopotential field (surfaces of constant $|H^2|$) and its gradient, the body force, were made nearly spherical by careful choice of magnet height-to-diameter ratio and magnet size relative to the PVC ball size. Terrestrial gravity is eliminated from Equation (1) by immersing

the “planet” and its ferrofluid “ocean” in an immiscible silicone oil/Freon mixture of the same density. Thus the earth gravity is removed from the dynamics of the ferrofluid/oil interface and the only dynamically active force there is the radial magnetic gravity. The entire apparatus can rotate, and waves are forced on the ferrofluid surface by exterior magnets.

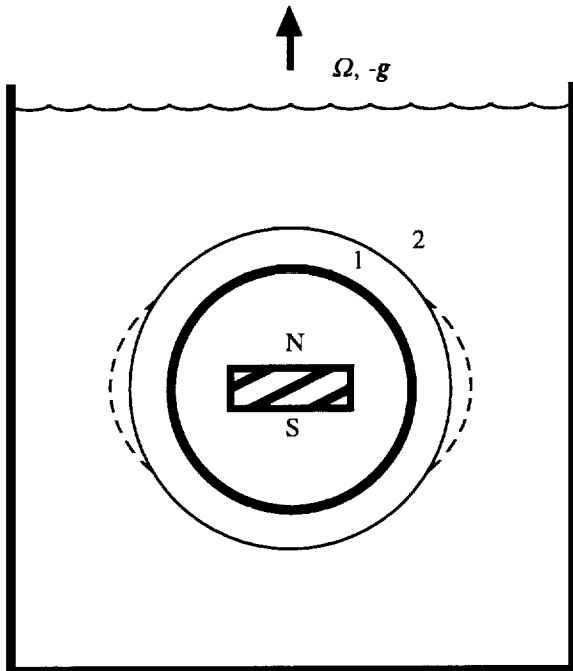


Figure 2. Side view schematic cross section of the cylindrically symmetric experiment. A cylindrical tank holds a silicone oil and Freon mixture (2) surrounding a water-based ferrofluid layer (1) that is held by the magnetic body force onto the surface of a PVC ball covering a cylindrical permanent magnet. $\rho_1 = \rho_2$ to eliminate terrestrial gravity. The entire apparatus rotates at angular frequency, Ω .

Figure 3 is a perspective view photograph of the apparatus. The external disk-shaped magnet at left forces a wave with maxima symmetrically displaced off the equator and a local minimum on the equator. Waves with a single maximum on the equator can be forced by inverting the forcing magnet polarity. A Plexiglas wall just visible on the right side in the black ferrofluid serves as a continental boundary for the ferrofluid ocean for studies of wave reflection discussed below. The entire ferrofluid ball is about 35cm in diameter, twice the size of reference [3], and the surrounding oil/Freon mixture has a viscosity 1/5 as large, giving more than an order of magnitude reduction in viscous effects. Careful temperature control of the water in the outer square box is required to maintain uniform density between the ferrofluid and oil/freon mixture as the expansion coefficients of the two fluids are different.

The biggest improvement in technique over [3] is in the wave visualization. Fluorescing dye is added to the oil/Freon mixture and an argon ion laser generates the horizontal light sheet visible in Figure 3. This sheet can be scanned vertically. Viewed from above, the experiment is a black circle with wave deformations surrounded by a light background. A contour of the image intensity at any light sheet position gives the surface of the ferrofluid “ocean” at that “latitude”. Radial displacements of the waves as a function of longitude are obtained by subtracting the contour line positions from a no-motion contour at that laser sheet latitude. The experiments are run by traversing the forcing magnet with the laser sheet height fixed and images are frame grabbed to obtain a time series at one latitude. The experiment is then re-run with another laser-sheet height to build up a full picture of the three-dimensional wave structure in the upper hemisphere of the ball as a function of time

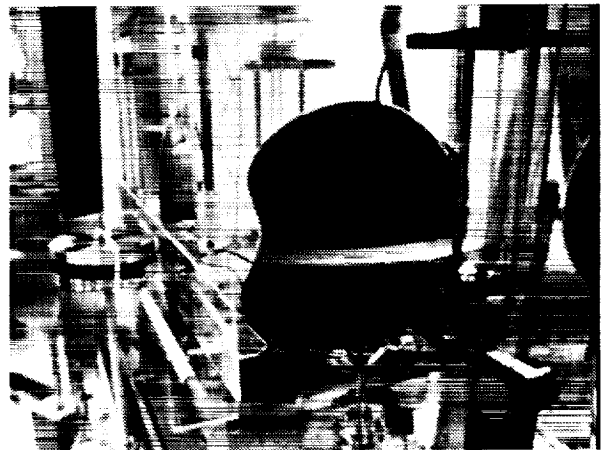


Figure 3. Photograph of the laboratory experiment. See text above for a description.

RESULTS

We concentrate here on results of laboratory studies of waves that are important in Earth’s atmosphere and especially the ocean. In large scale atmospheric and oceanic fluid dynamics, only the local vertical projection of the planetary rotation, $f = 2\Omega\sin(\text{latitude})$, is important because the atmosphere and ocean are very thin compared to their horizontal extent and stratification effects further inhibit vertical motions. An important class of waves in geophysical fluid dynamics depends on the latitudinal variation of f [4, 5]. These Rossby waves are evident for example in the structure and dynamics of the atmospheric jet stream and Atlantic Gulf Stream. At the equator f changes sign, and a special class of these waves is trapped to equatorial latitudes but carry energy and momentum east and west [5]. These equatorial Kelvin and Rossby waves are an integral part of the dynamics of El Niño. This ferrofluid experimental technique is the only laboratory realization of these equatorial waves. To get oceanic

scaling in the laboratory, the experiment must rotate rapidly (4-second rotation period) so that the wave speed is slow compared to the planetary rotation speed as in the ocean.

In [3] observations of equatorial Kelvin and Rossby waves were compared to theoretical predictions [4, 5] and satellite observations [6, 7]. These experiments were conducted on the full sphere with visualization of wave height only on the equator. Using the improved experiment with lower friction and better visualization, we have extended the results in [3] to verify the latitudinal shape of the westward propagating equatorial Rossby waves. These waves have their largest signal off the equator, something like the wave shown in Figure 3.

In the Pacific Ocean, eastward propagating Kelvin waves eventually run into the South American coast. Theory predicts that some of the wave energy should scatter into coastal-trapped Kelvin waves that propagate north and south along the coast [8]. Some of this coastal wave energy might then scatter into *mid-latitude* Rossby waves that propagate back westward. Satellite observations of the Pacific Ocean sea-surface temperature and height seem to show signatures of westward propagating Rossby waves at 20N to 50N latitude, 5 to 10 years after the 1982-83 El Niño [9]. The observational data is difficult to interpret unambiguously owing to the large range of motions that fill the ocean at shorter timescales.

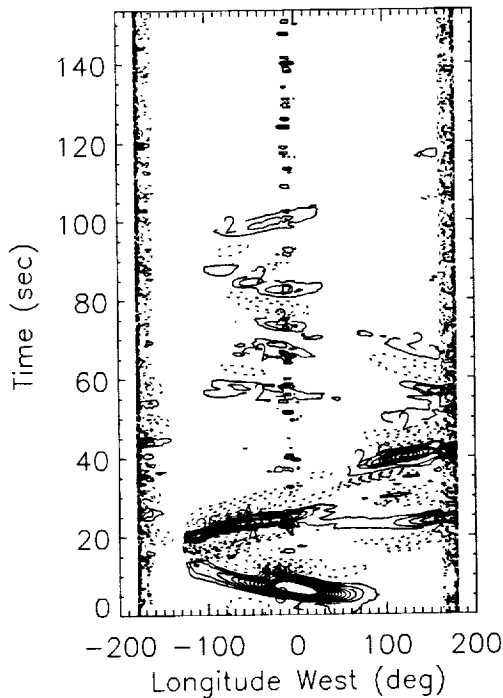


Figure 4. Wave height at 0°N latitude for non-rotating experiment.

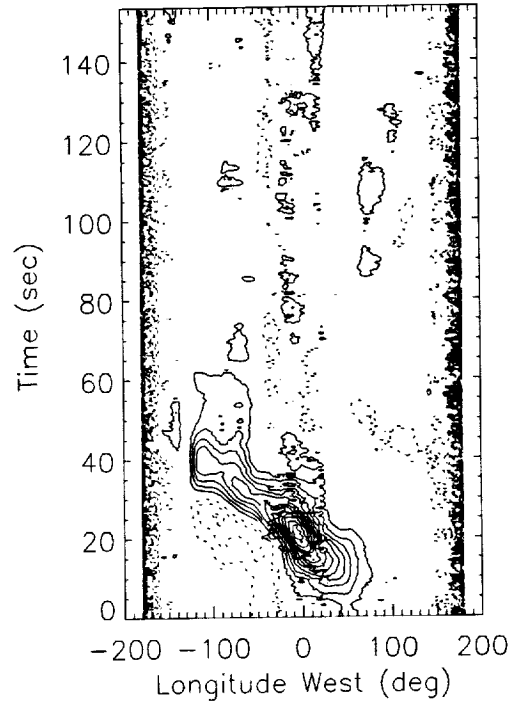


Figure 5. Wave height at 0°N latitude for 4-second rotation period experiment.

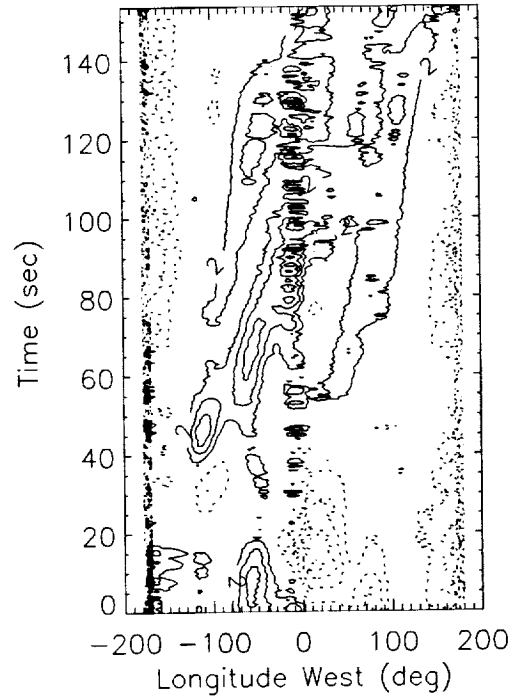


Figure 6. Wave height at 60°N latitude for 4-second rotation period experiment.

This series of reflections giving eastward, northward, and then westward traveling waves is observed cleanly in the laboratory experiments, confirming the theoretical expectations. Figures 4, 5, and 6 are all contours of wave height vs. longitude and time for experiments with a vertical wall (continent) placed at longitude -130°W . In the experiments, a wave with maximum amplitude on the equator is forced by an external magnet moving in the co-rotating direction (eastward). The magnet is closest to the experiment at 0°W longitude. Gaps in the laser-light sheet projection system give rise to the contour noise from -20°W to 10°W and 160°W to -170°W longitudes. In Figure 4 the experiment is not rotating and the wave height on the equator is plotted. The wave reflects from the wall and propagates at the same speed back to the west. Much of the wave energy propagates toward the pole in the non-rotating case (not shown). In contrast for the rapidly rotating case (Figures 5 and 6), the eastward wave propagates to the wall along the equator in Figure 5 and then disappears at about 40 seconds. Plots at higher latitude show the wave propagating northward until in Figure 6 at 60°N , the wave reaches maximum amplitude along the wall at 45 seconds and then propagates westward, more slowly than the eastward wave. This westward propagation at speeds slower than the equatorial Kelvin wave speed fits the classic long Rossby wave signature.

FUTURE WORK

The linear and nonlinear characteristics of traveling or standing waves on a liquid surface are a classic problem in fluid dynamics. Lateral boundaries have a strong effect on the spatial structures (fronts, pulses, solitons, etc.) observed in nonlinear propagating wave systems [10, for an extensive review]. It is of great theoretical interest to contrast wave behavior with and without lateral boundaries. With our spherical magnetic body force, a straight circumferential channel formed by boundaries at \pm latitudes is an experimental system for free-surface capillary-gravity waves that has periodic boundary conditions in one direction. Similarly, the entire spherical surface is boundary-less and periodic in two-dimensions. In an equatorial channel geometry, the contact lines are of the same length (as opposed to in an annular geometry) and this symmetry makes comparison to theory easier. We plan next to study various capillary-gravity waves using this apparatus which is the laboratory version of the standard theoretical periodic-boundary construct.

Standing capillary-gravity waves are excited if the gravitational force oscillates in time. This is normally accomplished by vibrating a fluid container vertically. These "Faraday waves" have become, along with Rayleigh-Benard convection, a canonical system for studies of non-equilibrium pattern formation, spatio-temporal evolution, and chaos [10]. Our spherical geometry, with parametric oscillation obtained by os-

cillating the magnetic field, is a very clean system for investigating such parametrically excited waves, without complications of boundary shapes and contact angles which can determine patterns and mode competition dynamics even very far from the boundaries [11]. We've designed an electromagnet version of the apparatus of Figures 2 and 3 to provide an oscillating "gravity". We should have sufficient electromagnetic driving strength in the frequency range 0.01 to 10 Hz, to generate Faraday wave patterns by parametric excitation with up to a few tens of waves in a circumference on the sphere or somewhat fewer fitting around inside a polar basin. The spherical system has the periodic boundaries of the standard theoretical development [11] but which have not been previously possible experimentally.

Continuing the geophysical applications, ferrofluid experiments offer the potential for conducting laboratory studies of thermally driven oceanic flows over a substantial part of a sphere. These slow deep overturning oceanic motions are highly constrained by the dynamical influence of planetary vorticity advection. Such effects cannot be studied in the terrestrial laboratory, when the all-important case of continuous thermal stratification is considered, because of the strong gravity induced cells that have no oceanic analogs. Previous GFFC-type [12] experiments are also ill suited to oceanic flow modeling because they are too viscous (thin gaps). We will address the key **technical** issues in building a relatively simple but effective microgravity based experiment to enable laboratory study of continuously stratified spherical flows in complex basins spanning a latitude range of at least plus or minus 60 degrees. We realize that such an experiment must be conducted in microgravity, and our terrestrial demonstration experiment will be contaminated by terrestrial gravity induced flows. The main technical issues to explore are: 1) how to get a large enough magnetic buoyancy frequency in an apparatus of sufficient size, 2) how to stratify and force motion in the experiments, and 3) how to visualize the flows effectively.

ACKNOWLEDGEMENTS

This work is supported by NASA grant NAG3-1848 and NSF grants OCE-9416661 and OCE-9709338. Scott Kittelman and Dr. Navid Borhani built the apparatus and Scott Kittelman has been instrumental in conducting all the experiments.

REFERENCES

1. Wang, T.G., A.V. Anilkumar, C.P. Lee, and K.C. Lin: *J. Fluid Mech.*, **276**, 389-403, 1994.
2. Rosensweig, R.E.: *Ferrohydrodynamics*. Cambridge University Press, 1985.
3. Ohlsen, D.R. and P.B. Rhines: *J. Fluid Mech.*, **338**, 35-58, 1997.

4. Gill, A.E.: *Atmosphere-Ocean Dynamics*. Academic Press, 1982.
5. Philander, S.G.: *El Niño, La Niña, and the Southern Oscillation*. Academic Press, 1990.
6. Chelton, D.B. and M.G. Schlax: *Science*, **272**, 234-238, 1996.
7. Delcroix, T., J. Picaut, and G. Eldin: *J. Geophys. Res.*, **96 (Suppl.)**, 3249-3262, 1991.
8. Clarke, A.J.: *J. Phys. Oceanogr.*, **13**, 1193-1207, 1983.
9. Jacobs, G.A., H.E. Hurlburt, J.C. Kindle, E.J. Metzger, J.L. Mitchell, W.J. Teague, and A.J. Wallcraft: *Nature*, **370**, 360-363, 1994.
10. Cross, M.C. and P.C. Hohenberg: *Rev. Mod. Phys.* **65**, 851-1112, 1993.
11. Miles, J. and D. Henderson: *Annu. Rev. Fluid Mech.*, **22**, 143-165, 1990.
12. Hart, J.E., G.A. Glatzmaier, and J. Toomre: *J. Fluid Mech.*, **173**, 519-544, 1986.